Plasma Turbulence Studies in ADITYA tokamak

R. Jha, P. Kaw, D. Raju, A. Sen and the ADITYA Team

Institute for Plasma Research, Bhat, Near Indira Bridge, Gandhinagar -382428, INDIA
Email of the main author: rjha@ipr.res.in

Abstract. A summary of results from measurements and analysis of edge turbulence in ADITYA tokamak is presented. The floating potential is found to be positive in the scrape-off layer as well as in the edge plasma with a minimum near the shear layer. The electrostatic Reynolds stress, estimated by a conditional averaging technique, is found to be highest near the shear layer. Measurements with gas-puff show strong suppression of edge fluctuations with concomitant reduction in Reynolds stress. The fluctuation data is further examined with a novel scheme of data analysis based on the `empirical mode decomposition' and Hilbert transform. It is found that the edge fluctuations can be well represented by a finite number of about 10 discrete modes. Their instantaneous energies show intermittent bursts and the high frequency modes are non-stationary. The technique is further developed to study three-mode interactions and employed to show that triplet interactions are statistically significant among high frequency modes of the fluctuation data.

1. Introduction

The study of edge fluctuations is an active area of research for fusion devices and is motivated by the desire to gain a better understanding and ultimately a better control of anomalous transport processes. In this paper, we present two of our recent efforts in this direction: one describing experimental measurements of Reynolds stress and the other related to characterization of fluctuation data using a Hilbert transform-based technique.

2. Measurement of Reynolds Stress

It is now widely recognized that the exchange of energy between large-scale sheared **ExB** mean flows and small-scale turbulent fluctuations is crucial for controlling anomalous heat and particle losses in fusion devices [1]. In order to gain a better understanding of this process, we have carried out measurements of the Reynolds stress (RS) experienced by turbulent eddies in the tokamak edge plasma. Measurements of RS are carried out in a normal flattop current plasma discharge as well as in conjunction with edge modification using gas-puff. For this purpose, a high throughput (500 SCCM) piezo-electric valve is mounted on a bottom port that is about 200 degrees from the probe system in the electron drift direction. The fluctuation measurements are carried out during 40-65 ms at the flattop plasma current. The piezo valve is opened for 1.7 ms and 4×10^{14} molecules of hydrogen gas are released into the plasma. Coinciding with the gas-puff, there is significant increase in the chord-averaged central plasma density, in the H_α emission and also in the soft X-ray emission [see Fig. (1)]. The quantity of the puffed gas is adjusted such that the plasma current and hence the plasma equilibrium is not affected significantly. It is observed that the gas-puff reduces potential fluctuation in the edge region but it does not cause significant reduction in density (or, ion saturation current) fluctuation. We have carried out measurements of radial profiles of floating potential with and without gas-puff to see if fluctuation suppression is caused by change in potential or **E×B** flow gradients. The electrostatic RS is determined from fluctuating velocity components in radial and poloidal directions.

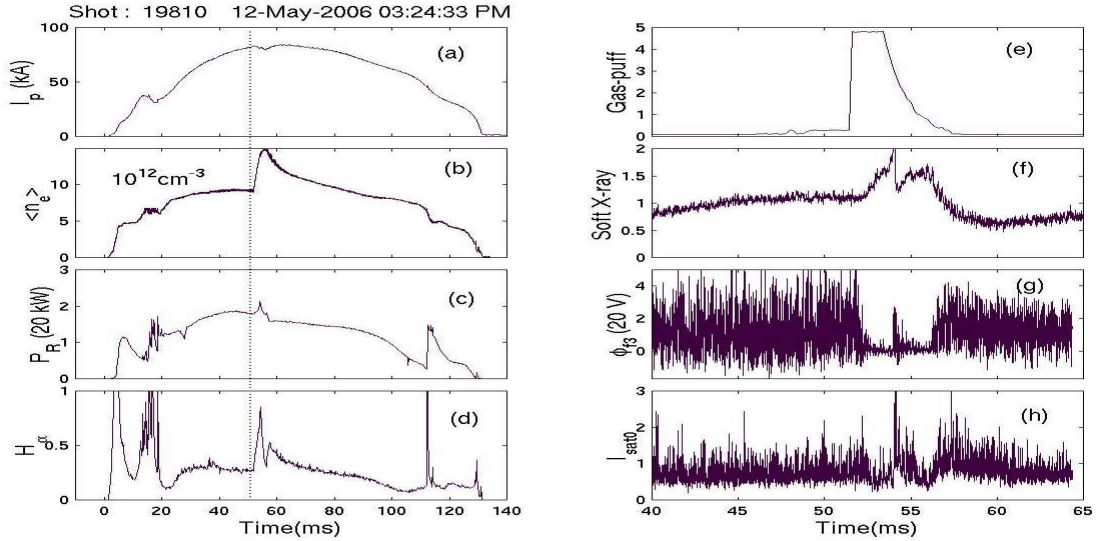

FIG. 1: Time-series of (a) plasma current, (b) chord-averaged plasma density, (c) bolometer signal and (d) H_α signal. The vertical dotted line indicates the time when gas-puff valve is opened. The blocks on the right shows: (e) Voltage on the gas-puff valve, (f) Soft X-ray, (g) floating potential and (h) ion-saturation current.

For this purpose, we use a set of nine Langmuir probes in cross (+) configuration: five probes spaced in the poloidal direction and another five in the radial direction, the central probe being common. This configuration is suitable for simultaneous measurement of radial and poloidal velocities experienced by a turbulent eddy. The probe system can be moved in the radial direction near the edge plasma and by collating data from many similar discharges it allows measurement of radial profiles of floating potential, **E×B** velocity, shear rate etc. Figure 2 shows the floating potential profile at a time when there is no gas-puff and that during the gas-puff. We note that the floating potential is positive in the edge as well as in the SOL plasma with a minimum near the separatrix. Figure 3 shows RMS (root mean square) values of fluctuation levels. It is observed that during the gas-puff when there is a suppression of fluctuation, the mean floating potential profile also gets flattened. However, both with and without gas-puff, the fluctuation level is minimum at radial distance between 0-20 mm from the separatrix. We have determined the radial profiles of **E×B** flow velocity as well as its gradient in both discharge conditions (i.e., with and without gas-puff). It is observed that near the shear layer, the maximum shear $\partial V_{E\times B}/\partial r \approx 4\times10^5\, s^{-1}$ in the normal discharge and $2\times10^5\, s^{-1}$ during the gas-puff.

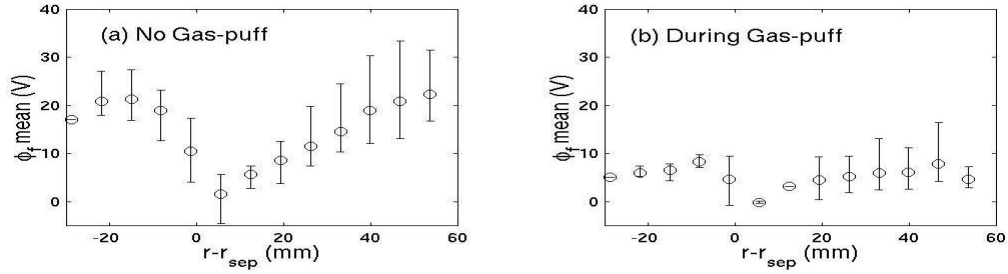

FIG. 2: Radial profiles of mean floating potential (a) without gas-puff, and (b) during gas-puff. The open circle shows the mean value over several discharges and error bar indicates the total spread.

These values are larger than the de-correlation frequency $10^5 s^{-1}$ and explain fluctuation suppression in the shear layer. We had expected that during gas-puff the velocity gradient would increase but we do not observe such a thing. In the present experiment, the duration of fluctuation suppression is small (5 ms compared to 2 ms confinement time). It is likely that gas-puff causes confinement improvement, but conclusive evidence can come only if we get fluctuation suppression for a longer time. Another point to study in detail will be to determine the cause of fluctuation suppression. Future experiments would be directed towards measurement of toroidal flow velocity using a Mach number probe.

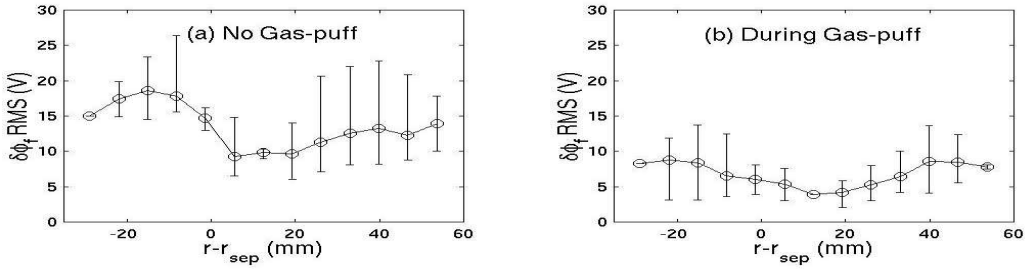

FIG. 3: Radial profile of the root mean square (RMS) value of potential fluctuations in discharges (a) without gas-puff and (b) during gas-puff.

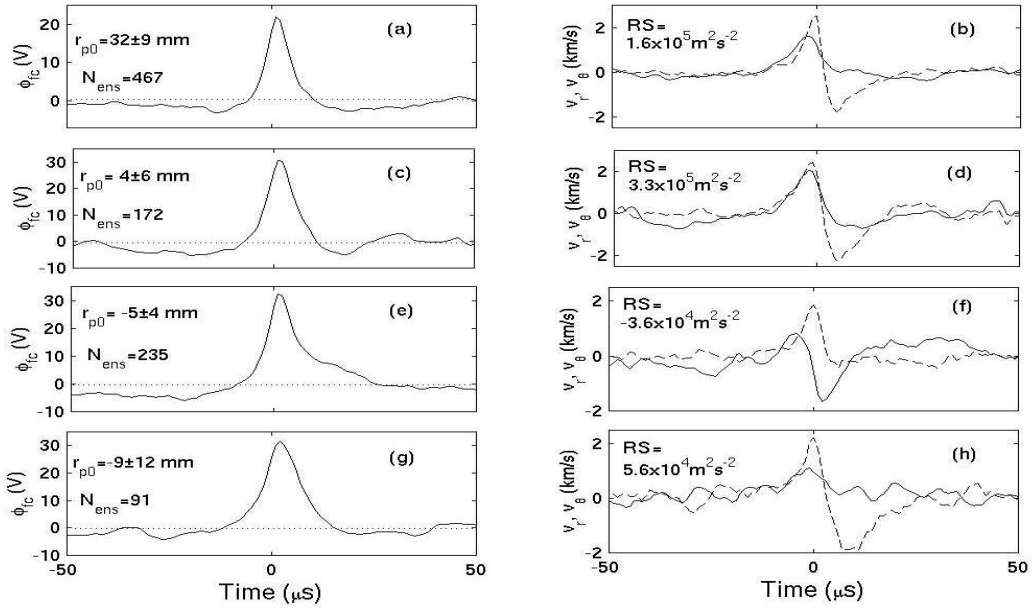

FIG. 4: (a), (c), (e) and (g) are ensemble averages of conditional eddies seen by the central probe at different radial locations, r_{p0} from the separatrix. Even when the probe is placed at a certain radial distance, its distance from the separatrix can be different in different discharges because of lack of position control. Figures (b), (d), (f) and (h) show conditionally averaged radial (δv_r) and poloidal (δv_θ) velocities. The estimates Reynolds stress, RS= $\langle \delta v_r \delta v_\theta \rangle$ is also shown.

In the turbulent edge plasma, the electrostatic RS (=$\langle \delta v_r \delta v_\theta \rangle$) represents radial flux of poloidal momentum and may be responsible for driving the mean flow. This is one of the mechanism by which the small-scale fluctuations can get suppressed. As a part of this study we have measured RS in a normal discharge. To improve accuracy, we had to use data from several discharges so that the number of ensembles [$N_{ens,}$ see Figure inset] is large. The data

length during gas-puff is too small to allow an unambiguous measurement of RS at different radial locations. For collecting ensembles, an eddy is picked up on the central pin of the cross (+) probe by imposing the following conditions: (i) the amplitude of the eddy exceeds 1.5σ above the mean level, and (ii) the slope ($\partial\phi_f / \partial t$) is positive. Other details of conditional averaging are same as in Ref. [2]. We also have simultaneous measurement of fluctuating radial velocity (δv_r) and poloidal velocity (δv_θ) experienced by the reference eddy. A large number of ensembles of these quantities are collected from the time-series. Figure 4 shows the ensemble averages of these quantities when the probe is placed at different radial distances from the separatrix [indicated in Figure *4(a,c,e,g)*]. The positive value of δv_r is in the outward and positive δv_θ indicates electron diamagnetic direction. It is observed that in the far-SOL (r_{p0}= 30±14 mm), eddies move radially outward but poloidal velocity is bipolar. One half of the eddy moves in electron diamagnetic direction and the other half in ion diamagnetic direction- indicating a spinning motion. It is noted that δv_r is outward in the SOL but inside the separatrics it is either negligibly small or directed inward. The values of RS are shown in Fig. *4(b,d,f,h).* It is observed that a strong gradient in the RS exists between the radial locations r_{p0}= 4±6 mm and r_{p0} = -5±4 mm from the separatrix, giving $\partial\langle\delta v_r \delta v_\theta\rangle / \partial r \approx 7\times10^7 m^1 s^{-2}$. Using the value of $\partial^2 V_{E\times B} / \partial r^2 \approx 7\times10^7 m^{-1} s^{-1}$ as derived from Fig. *2(a)* in the shear region, one obtains viscosity $\eta_{\exp} \approx 1 m^2 s^{-1}$. Future experiments will now focus on increasing the duration of fluctuation suppression with gas-puff and studying relations between flows and turbulence.

3. Hilbert transform based tokamak data analysis

To obtain further insight into the turbulence characteristics we have analyzed the fluctuation data using a novel technique based on the Hilbert transform developed by Huang *et al.* [3]. The method has two major components - a shifting process known as 'empirical mode decomposition' that extracts a finite number of mono-frequency modes (the intrinsic mode functions, IMFs) and subsequent application of the Hilbert transform on the IMFs that permits evaluation of instantaneous frequencies and amplitudes. In contrast to Fourier transform-based techniques, the present method can be applied to non-stationary data as well as to data sets that have a relatively small number of data points. The method is also superior to wavelet-based techniques in many respects. A detailed description of this technique and its application on tokamak data has been presented in Ref. [4]. Here we describe some key results that illustrate the strength of this technique. The Hilbert transform of an IMF *X(t)* can be written as:

$$Y(t) = \frac{1}{\pi} \mathrm{P} \int_{-\infty}^{+\infty} \frac{X(\tau)}{t-\tau} d\tau \qquad \ldots.(1)$$

where, *P* is the Cauchy principal value of the integral. By taking Fourier transforms of *X(t)* and *Y(t),* it can be shown that $Y(\omega) = -jX(\omega)$. Thus, all frequency components of *Y(t)* are delayed in phase by π/2 and hence are orthogonal to *X(t).* The analytic signal, $Z(t) = X(t) + jY(t)$ allows an appropriate definition of instantaneous amplitude, $A(t) = \sqrt{X^2 + Y^2}$ also known as the envelope, and instantaneous phase $\Theta(t) = \tan^{-1}(Y/X)$. The instantaneous angular frequency $\omega(t)$ is the local slope of $\Theta(t)$. When we analyze edge fluctuation data using this technique, we find that the edge fluctuation data contain a finite number of IMFs in contrast to the huge number of modes that a Fourier transform analysis

would yield. Some of these modes are not correlated with the raw data, and hence they are spurious. The physically relevant modes are those that are correlated with the raw data with a normalized correlation coefficient of > 10 %. These are physically relevant modes and hence they can be used for further analysis.

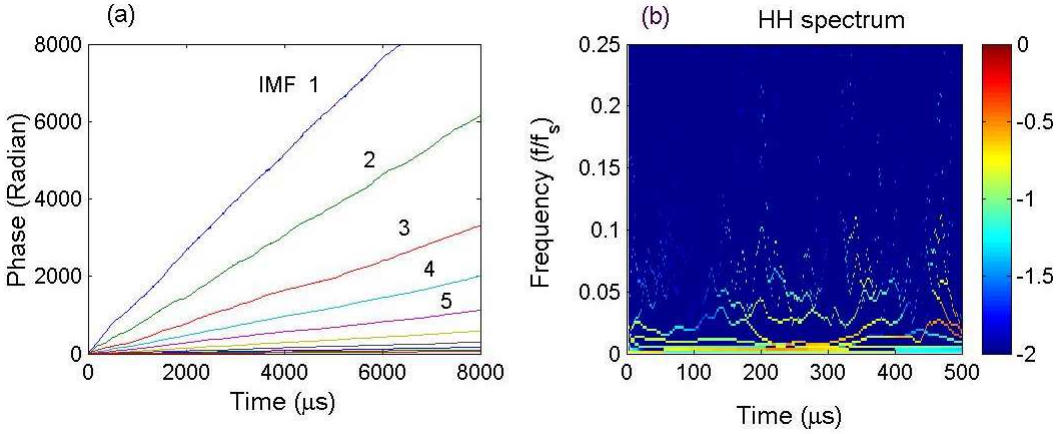

FIG. 5: (a) Un-wrapped phases of IMF components of ϕ_f data, and (b) Hilbert-Huang (HH) spectrum of a small segment of the data. The colored dots represent the variation of amplitude on a time frequency plot (the HH spectrum).

Figure 5(a) shows the instantaneous phases of these modes and the mean frequency of a mode is nearly constant. However undulation on a phase clearly shows that instantaneous frequency wanders around the mean frequency. The mode amplitude can be represented on time-frequency plane and such a representation is known as Hilbert-Huang (HH) spectrum, $H(t,\omega) = \mathrm{Re}\sum_i A_i(t)\exp[j\int \omega_i(t)dt$ where the summation is over the relevant IMFs. Figure 5(b) shows the HH spectrum for fluctuation data and it is characterized by intermittent variation of instantaneous frequency.

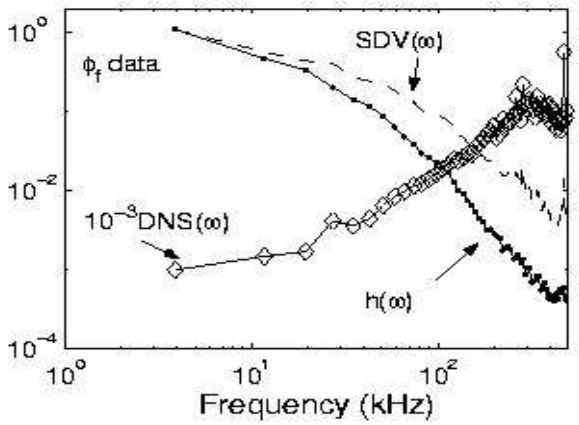

FIG. 6: The mean marginal spectrum h(ω), the deviation spectrum SDV(ω) and the degree of non-stationarity spectrum DNS(ω) of the ϕ_f data from ADITYA SOL plasma. The deviations from the mean marginal spectrum and the degree of non-stationarity are higher for higher frequency components.

The HH spectrum can be used to extract several integral or averaged quantities that are sensitive measures of turbulence characteristics. One such measure is the mean marginal spectrum, $h(\omega)$ which is comparable to the Fourier spectrum but more meaningful because it is based of the empirical modes present in the data. Likewise, another integral quantity, the degree of non-stationarity (DNS), shows how different frequency components deviate from

the mean marginal spectrum. The deviation spectrum $SDV(\omega)$ is shown in Fig. (6) along with $DNS(\omega)$. It is observed that the low frequency modes ($< 20\ kHz$) are nearly stationary, but higher frequency modes become non-stationary. This conclusion can also be made from the visual inspection of different IMFs.

We have further generalized this technique to explore the occurrence of phase coupling in the turbulence data. The basic idea is to associate the IMFs as the basic nonlinear modes of the system and examine their mutual interactions. Since IMF components are represented as, $Z_i(t) = A_i(t)\exp[j\Theta(t)]$, interactions among them can be studied by evaluating the IMF bi-coherency factor, namely,

$$\gamma = \frac{\langle Z^*_i Z_{i+1} Z_{i+2} \rangle}{\langle A_i A_{i+1} A_{i+2} \rangle} \qquad \ldots.(2)$$

where, the angular bracket represents time averaging. If the phases, Θ_i, Θ_{i+1}, and Θ_{i+2} are random, the numerator $\langle Z_i^* Z_{i+1} Z_{i+2} \rangle \approx 0$ and if $\Theta_i = \Theta_{i+1} + \Theta_{i+2}$, the numerator is equal to $\langle A_i A_{i+1} A_{i=2} \rangle$. Thus, the bi-coherency factor γ is bound in the range [0,1] and it can be used to detect phase coupling. The error $\varepsilon(\gamma)$ is estimated by counting the number (M) of the largest wave in the triplet (i.e., the number of 2π phases). It is assumed that each wave period is independent and thus M represents the number of independent ensembles for averaging so that the error, $\sigma(\gamma) = 1/\sqrt{M}$.

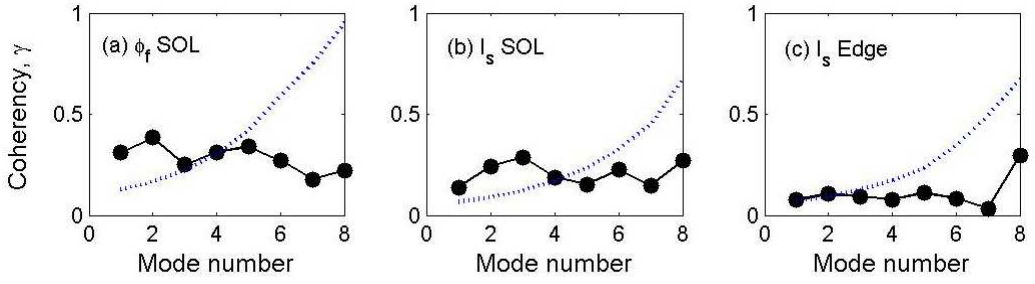

FIG. 7: The coherency factor of triplet coupling in three data sets obtained from the ADITYA tokamak, (a) floating potential (ϕ_f) data from the SOL plasma, (b) ion saturation current (I_s) data from the SOL plasma and (c) the I_s data from the edge plasma (6 mm into the main plasma). The dotted line indicates 3σ error in the estimates of the coherency factor, γ.

Figure 7 shows measurement of IMF bi-coherency for three data sets of fluctuations in the SOL and edge plasmas. It is observed that the IMF bi-coherency is statistically significant among a few high frequency modes in the SOL plasma but the edge plasma close to the limiter has negligible triplet coherency. This is consistent with the widely accepted notion that the edge plasma behind the limiter has a velocity shear layer which can de-correlate turbulent fluctuations whereas the SOL plasma is rich in coherent structures.

The *HH* spectrum can be used to estimate the instantaneous energy, $IE(t) = \sum_\omega H^2(t,\omega)$, which truthfully tracks the fluctuation activity in the time-series. Since this quantity is dominated by low frequency modes, the *IE* demonstrates the time-scales of modulation energy present in the data. We have estimated *IE* for the edge fluctuation data and observe that it correlates with the fluctuation activity and has a characteristic time-scale of about 200

μs. This can be compared with the auto-correlation time of the fluctuation that is about 10 μs. Thus, the energy of edge turbulence modulates at a time-scale that is 20 times larger than the time-scales of turbulent fluctuation.

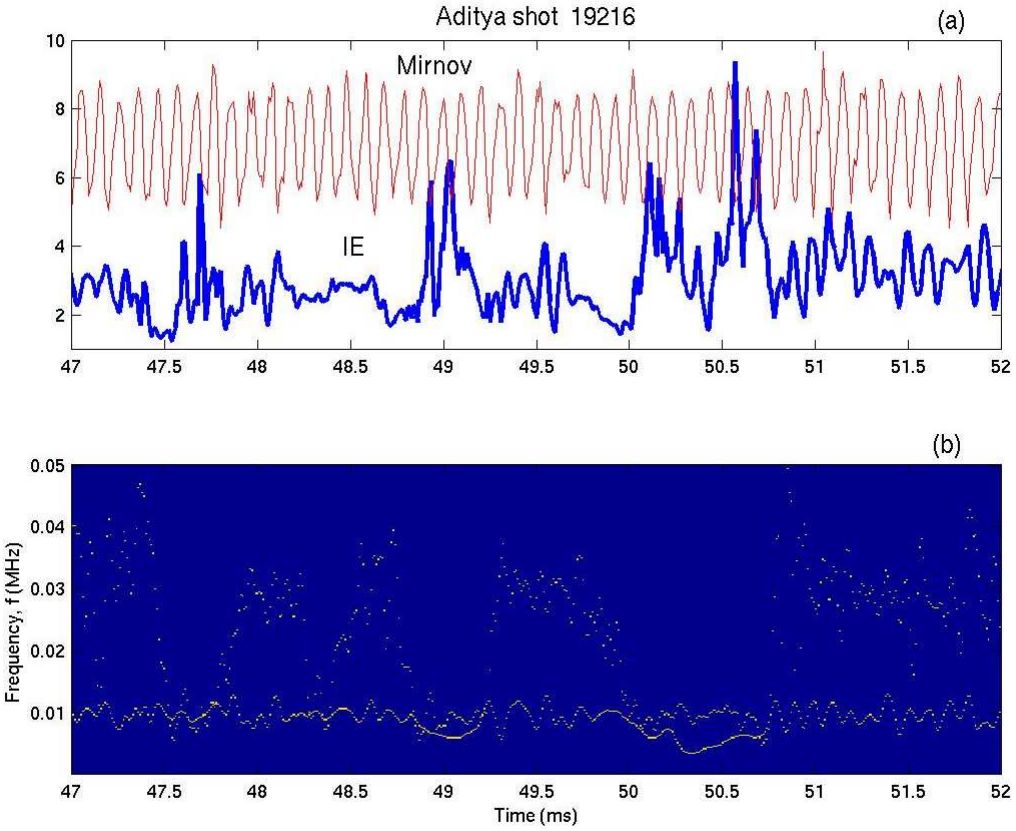

FIG. 8: The Mirnov coil data, dB_θ/dt in ADITYA tokamak and the instantaneous energy (IE) during plasma current flattop, and (b) its Hilbert-Huang spectrum taking only the first two IMFs.

We have also carried out similar measurements for the Mirnov coil data. When the magnetic oscillation data are decomposed into IMFs, we find that only two of the several IMFs are strongly correlated with the raw data. These modes have mean frequency of 10 kHz and 30 kHz respectively. The HH spectrum and the instantaneous energy (IE) are obtained from these modes. To facilitate easy interpretation, only Mirnov data during plasma current flattop is used when we expect mean plasma pressure profile to have been well established. We observe that whenever IE is large, there is only one frequency component at 10 kHz [see Fig. 8(a), and 8(b)]. However, in between successive events of high IE, there are periods of low IEs when the second frequency at about 30 kHz also appears. The intermittent bursting of the high frequency component (the second IMF) would not have been physically significant if the IE was close to zero. A significant level of IE at the time of the high frequency bursts implies that this phenomenon has a physical origin. As is well known, the mode frequency of a Mirnov oscillation is related to the plasma diamagnetic frequency that in turn depends on the plasma pressure gradient. The bursts in high frequency components can therefore be interpreted as being due to intermittent changes in the local plasma pressure gradient - reminiscent of sand-pile avalanches that maintain profile consistency.

Reference:

[1] E. Sanchez, C. Hidalgo, B. Gonzalves et al., J. Nucl. Mater. **337-339**, 296 (2005).
[2] B. K. Joseph, R. Jha, P. K. Kaw et al., Phys. Plasmas **4**, 4292 (1997).
[3] N. E. Huang, M. C. Wu, S. R. Long et al. Proc. R. Soc. London A **459**, 2317 (2003).
[4] R. Jha, D. Raju and A. Sen, Phys. Plasmas **13**, 82507 (2006).